A New Approach for Estimating Tire-Road Longitudinal Forces for a Race Car

DELL'ANNUNZIATA, GN, LENZO, Basilio <http://orcid.org/0000-0002-8520-7953>, FARRONI, F, SAKHNEVYCH, A and TIMPONE, F

Published version

DELL'ANNUNZIATA, GN, LENZO, Basilio, FARRONI, F, SAKHNEVYCH, A and TIMPONE, F (2019). A New Approach for Estimating Tire-Road Longitudinal Forces for a Race Car. In: UHL, Tadeusz, (ed.) Advances in Mechanism and Machine Science: Proceedings of the 15th IFToMM World Congress on Mechanism and Machine Science. Mechanisms and Machine Science (73). Springer, 3601-3610.

A New Approach for Estimating Tire-Road Longitudinal Forces for a Race Car

Guido Napolitano Dell'Annunziata[1,2], Basilio Lenzo[1*], Flavio Farroni[2], Aleksandr Sakhnevych[2], Francesco Timpone[2]

[1] Sheffield Hallam University, S11WB, Sheffield, United Kingdom
[2] Università degli studi di Napoli Federico II, 80125, Naples, Italy
basilio.lenzo@shu.ac.uk

Abstract. In vehicle dynamics, the determination of the tire-road interaction forces plays a fundamental role in the analysis of vehicle behavior. This paper proposes a simple yet effective approach to estimate longitudinal forces. The proposed approach: i) is based on equilibrium equations; ii) analyses the peculiarities of driving and braking phases; iii) takes into account the interactions between vehicle sprung mass and unsprung mass. The unsprung mass is often neglected but that might lead to significant approximations, which are deemed unacceptable in performance or motorsport environments. The effectiveness of the proposed approach is assessed using experimental data obtained from a high performance racing car. Results show that the proposed approach estimates tire longitudinal forces with differences up to 10% when compared against a simpler formulation which uses only the overall mass of the vehicle. Therefore the distinction among vehicle sprung and unsprung masses, which is likely to be an easily obtainable piece of information in motorsport environments, is exploited in this approach to provide significant benefits in terms of longitudinal force estimation, ultimately aimed at maximizing vehicle performance.

Keywords: Vehicle Dynamics, Tire-Road Interaction, Longitudinal Forces, Sprung and Unsprung Masses.

1 Introduction

The accurate estimation of the tire-road interaction forces is of great interest in vehicle dynamics. Only through a precise and accurate calculation of such forces the real behavior of the vehicle can be thoroughly investigated, understanding whether the tires are working correctly and at the maximum of their performance.

In recent years, tire technological development has played a fundamental role in motorsport and in the automotive sector. The availability of reliable procedures and methods to estimate tire-road interaction forces is a crucial aspect therein.

In the literature several contributions [1-5] deal with this problem, using different hypotheses and schematizations of the vehicle. In most cases, a single-track model is introduced, but that is not suitable to calculate the forces on each corner. Other ap-

proaches adopt Kalman filters to calculate tire-road interaction forces [6-8]. In [9] the T.R.I.C.K. tool is presented, which uses a 8 degrees-of-freedom (DOF) rear-wheel-drive vehicle model to obtain a fairly good estimation of the tire-road interaction forces. However, only the global mass of the vehicle is considered, without looking in detail at sprung mass and unsprung mass. In [10], sprung and unsprung masses are used to develop a tool that calculates the energy released from a vehicle to the road pavement, but such data are not directly used to estimate the interaction forces.

The main novelty of this paper is to present a formulation for the calculation of longitudinal forces that takes into account the distribution of the vehicle global mass into sprung mass and unsprung mass. The availability of such information is not a difficult task especially in motorsport environments, and it allows to introduce a significantly improved accuracy in the estimation of the tire-road longitudinal forces. Also, a different approach is used when compared to [9], i.e. individual free body diagrams are studied and exploited in the present formulation, which leads to different results than [9] even when only the global mass of the vehicle is considered. Additionally, in most road vehicles a further distinction can be made between the unsprung mass of the front wheels and the rear wheels, e.g. for a rear-wheel drive architecture, the rear wheel assembly includes additional components for housing the axle shafts.

Section 2 introduces the equilibrium equations of the individual wheels and of the whole vehicle, leading to two formulations. Section 3 investigates the general case of a non-even front-rear distribution of unsprung mass. In Section 4 the proposed formulations are assessed via experimental data acquired on a high-performance race car.

2 Longitudinal Force Formulations

The reference system used to calculate the longitudinal forces is the same as in [1]: it is centered in the vehicle center of mass, x is the longitudinal axis, positive forwards, y is the lateral axis, positive to the left, and z is the vertical axis, positive upwards. Table 1 reports the list of symbols used throughout the paper. The vehicle is assumed to be rear-wheel-drive, also it is assumed $a_x > 0$ and $F_x < 0$ in the direction of travel.

Acceleration and braking cases need to be addressed separately because of their individual peculiarities. Two main formulations are presented:

1. Splitted Mass Formulation (SMF), considering sprung mass and unsprung mass;
2. Overall Mass Formulation (OMF), considering only the total mass of the vehicle.

2.1 SMF - Acceleration

Based on individual free body diagrams, the equilibrium equations can be derived.

Front Wheel (Fig. 1a)

– Moment balance equation (rotation around the wheel center):

$$F_{xT1j}R_1 + F_{RR1j}R_1 - F_{z1j}t_1 = J_{z1}\ddot{\theta}_{1j} \quad (1)$$

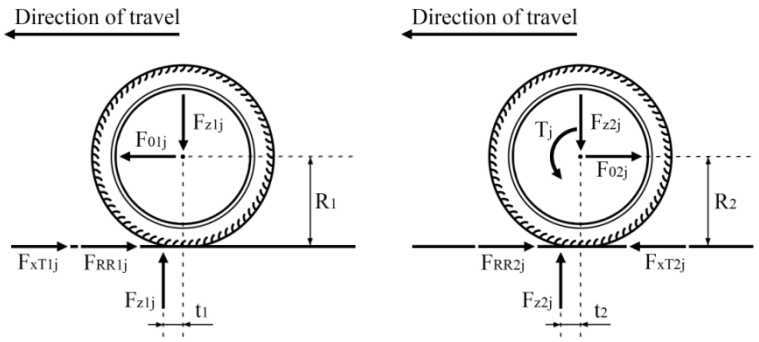

(a) (b)

Fig. 1. Acceleration: (a) front wheel, (b) rear wheel

Table 1. List of symbols

Symbol	**Description**
a_x	Vehicle longitudinal acceleration
$F_{Aerodrag}$	Drag force
F_{RRij}	Rolling resistance for wheel ij
F_{xij}	Overall tire-road longitudinal interaction force for wheel ij
F_{xTij}	Tire-road longitudinal interaction force for wheel ij, excluding F_{RRij}
F_{zij}	Vertical load for wheel ij
F_{0ij}	Force transmitted to the hub for wheel ij
J_{zi}	Moment of inertia for wheel i
M_{ij}	Braking torque action for wheel ij
m	Overall vehicle mass
m_R	Unsprung mass
m_{RF}	Front wheel unsprung mass
m_{RR}	Rear wheel unsprung mass
m_v	Sprung mass
R_i	Effective rolling radius for wheel i
T	Driving torque
T_j	Driving torque acting on a single wheel j
t_i	Offset between F_{zij} contributions due to rolling resistance
γ_j	Vertical force distribution (rear left - rear right)
δ	Vertical force distribution (front-rear)
$\ddot{\theta}_{ij}$	Angular acceleration for wheel ij
Subscripts	
i axle index: 1=front, 2= rear	j Side index: 1=left, 2=right

– Longitudinal equilibrium equation:

$$-F_{01j} + F_{xT1j} + F_{RR1j} = -m_R a_x \quad (2)$$

The reaction force F_{z1j} from the road to the vehicle is shifted forwards by t_1 with respect to the wheel center, due to rolling resistance, so that $F_{RR1j}R_1 = F_{z1j}t_1$. Therefore Eq. (1) can be rearranged as:

$$F_{xT1j} = J_{z1}\frac{\ddot{\theta_{1J}}}{R_1} \tag{3}$$

The longitudinal force exchanged between tire and wheel 1j is $F_{xT1j} + F_{RR1j}$:

$$F_{x1j} = F_{xT1j} + F_{RR1j} = J_{z1}\frac{\ddot{\theta_{1J}}}{R_1} + F_{RR1j} \tag{4}$$

Combining Eq. (2) and (4), the force transmitted to the hub for wheel 1j is:

$$F_{01j} = m_R a_x + J_{z1}\frac{\ddot{\theta_{1J}}}{R_1} + F_{RR1j} \tag{5}$$

Sprung mass (Fig. 2)

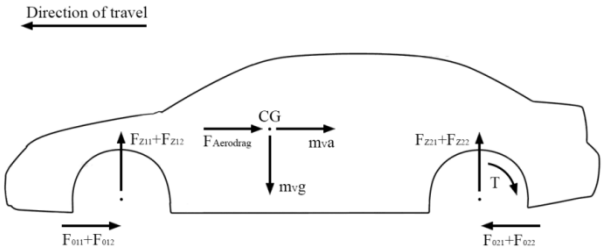

Fig. 2. Acceleration: sprung mass

– Longitudinal equilibrium equation:

$$F_{Aerodrag} + F_{011} + F_{012} - F_{021} - F_{022} = -m_v a_x \tag{6}$$

$F_{Aerodrag}$ is assumed applied at the vehicle center of mass, which is an approximation [1], however that has a negligible effect the estimation of the longitudinal forces. Equation (6) can be rewritten in the following form, useful to obtain Eq. (11) later:

$$F_{021} + F_{022} = m_v a_x + F_{Aerodrag} + F_{011} + F_{012} \tag{7}$$

The moment balance equation is not studied as it only provides information about the vehicle pitch motion, with no effect on the estimation of the longitudinal forces.

Rear Wheel (Fig. 1b)

– Longitudinal equilibrium equation:

$$F_{02j} + F_{RR2j} - F_{xT2j} = -m_R a_x \tag{8}$$

– Moment balance equation (rotation around the wheel center):

$$T_j + F_{RR2j}R_2 - F_{z2j}t_2 - F_{xT2j}R_2 = J_{z2}\ddot{\theta}_{2j} \tag{9}$$

The longitudinal force exchanged between tire and wheel 2j is $-F_{xT2j} + F_{RR2j}$:

$$F_{x2j} = F_{RR2j} - F_{xT2j} = -m_R a_x - F_{02j} \quad (10)$$

Replacing F_{02j} from Eq. (7), using Eq. (5) and introducing $\gamma_j = \frac{F_{z2j}}{F_{z21}+F_{z22}}$:

$$F_{x2j} = -m_R a_x - \left(m_v a_x + F_{Aerodrag} + 2m_R a_x + J_{z1}\left(\frac{\ddot{\vartheta}_{11}}{R_1} + \frac{\ddot{\vartheta}_{12}}{R_1}\right) + F_{RR11} + F_{RR12}\right)\gamma_j \quad (11)$$

The overall $F_{021} + F_{022}$ contribution is split based on the vertical loads at left and right side, using γ_j, whenever no information is available on the differential, following the approach in [9] which accounts for longitudinal and lateral load transfers as well as downforce.

2.2 OMF and comparison with SMF - Acceleration

The OMF formulation is here introduced, for use when no specific data on sprung and unsprung mass are available. For the front wheels still Eq. (4) holds, whilst for the rear wheels the OMF formula is:

$$F_{x2j} = -\left(ma_x + F_{Aerodrag} + J_{z1}\frac{\ddot{\theta}_{11}}{R_f} + J_{z1}\frac{\ddot{\theta}_{12}}{R_f} + F_{RR11} + F_{RR12}\right)\gamma_j \quad (12)$$

The inertia and rolling resistance contributions are the same in Eq. (11) and Eq. (12). Differences arise in all terms containing a mass: Table 2 compares such terms for SMF and OMF, for three values of γ_j. It should be noted that $m = m_v + 4m_R$.

Table 2. Comparison between SMF and OMF for rear wheels - Acceleration

γ_j	SMF term(s)	OMF term(s)	Magnitude
0	$-m_R a_x$	0	|SMF| > |OMF|
0.5	$-2m_R a_x - m_v a_x/2$	$-2m_R a_x - m_v a_x/2$	|SMF|= |OMF|
1	$-3m_R a_x - m_v a_x$	$-4m_R a_x - m_v a_x$	|SMF| < |OMF|

The OMF introduces an error which depends on the vertical loads on the wheel. In particular, the error grows when the vertical loads are different from each other, which is typical of lateral dynamics. If $\gamma_j \in [0; 1/2[$ the OMF underestimates the longitudinal forces. If $\gamma_j \in]1/2; 1]$ the OMF overestimates the longitudinal forces.

2.3 SMF - Braking

Sprung mass (Fig. 3)

— Longitudinal equilibrium equation:

$$F_{Aerodrag} + F_{011} + F_{012} + F_{021} + F_{022} = -m_v a_x \quad (13)$$

which can be rewritten as:

$$F_{011} + F_{012} + F_{021} + F_{022} = -m_v a_x - F_{Aerodrag} \quad (14)$$

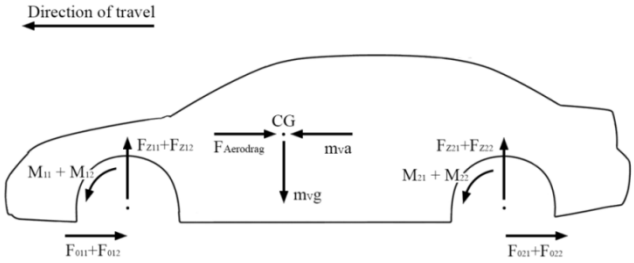

Fig. 3. Braking: sprung mass

Front Wheel (Fig. 4)

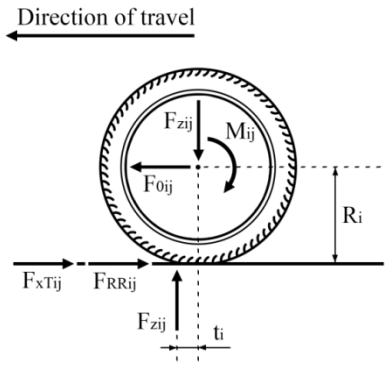

Fig. 4. Braking: generic wheel

– Moment balance equation (rotation around the wheel center):

$$F_{xT1j}R_1 + F_{RR1j}R_1 - F_{z1j}t_1 - M_{1j} = J_{z1}\ddot{\theta}_{1j} \quad (15)$$

– Longitudinal equilibrium equation:

$$-F_{01j} + F_{xT1j} + F_{RR1j} = -m_R a_x \quad (16)$$

Introducing $\delta = \frac{F_{z11}+F_{z12}}{F_{z11}+F_{z12}+F_{z21}+F_{z22}}$, from Eq. (14):

$$F_{01j} = (-m_v a_x - F_{Aerodrag})\frac{\delta}{2} \quad (17)$$

where the factor 2 indicates a 50-50 left-right distribution of the braking effort.

The longitudinal force exchanged between tire and wheel 1j is $F_{xT1j} + F_{RR1j}$:

$$F_{x1j} = F_{xT1j} + F_{RR1j} = -m_R a_x + (-m_v a_x - F_{Aerodrag})\frac{\delta}{2} \quad (18)$$

Rear Wheel (Fig. 4)

Following from Eq. (18) and from the definition of δ:

$$F_{x2j} = F_{xT2j} + F_{RR2j} = -m_R a_x + (-m_v a_x - F_{Aerodrag})\frac{(1-\delta)}{2} \quad (19)$$

2.4 OMF and comparison with SMF - Braking

OMF does not account for sprung and unsprung masses, therefore:

$$F_{x1j} = (-ma_x - F_{Aerodrag})\frac{\delta}{2} \quad (20)$$

$$F_{x2j} = (-ma_x - F_{Aerodrag})\frac{(1-\delta)}{2} \quad (21)$$

Table 3. Comparison between SMF and OMF for front wheels - Braking

δ	SMF term(s)	OMF term(s)	Magnitude
0	$-m_R a_x$	0	|SMF| > |OMF|
0.5	$-m_R a_x - m_v a_x/4$	$-m_R a_x - m_v a_x/4$	|SMF| = |OMF|
1	$-m_R a_x - m_v a_x/2$	$-2m_R a_x - m_v a_x/2$	|SMF| < |OMF|

Table 4. Comparison between SMF and OMF for rear wheels - Braking

δ	SMF term(s)	OMF term(s)	Magnitude
0	$-m_R a_x - m_v a_x/2$	$-2m_R a_x - m_v a_x/2$	|SMF| < |OMF|
0.5	$-m_R a_x - m_v a_x/4$	$-m_R a_x - m_v a_x/4$	|SMF| = |OMF|
1	$-m_R a_x$	0	|SMF| > |OMF|

Table 3 and Table 4 compare SMF and OMF in braking, for three values of δ. SMF and OMF coincide only if $\delta = 0.5$. If $\delta \in [0; 1/2[$ the OMF underestimates the longitudinal forces for the front wheels and overestimates them for the rear wheels. If $\delta \in]1/2; 1]$ the OMF overestimates the longitudinal forces for the front wheels and underestimates them for rear wheels.

3 SMF with Different Unsprung Masses: SMF*

This paragraph studies presents the case in which front and rear unsprung masses are different. As discussed before, such a condition is not unlikely, e.g. depending on the drive architecture, the front and rear wheel assemblies may differ significantly. This formulation will be indicated as SMF*. It implies $m = m_v + 2m_{RF} + 2m_{RR}$.

During acceleration, SMF* and the OMF are identical for the front wheels. For the rear wheels, replacing m_R with m_{RF} and m_{RR} where appropriate in Eq. (11):

$$F_{x2j} = -m_{RR}a_x - \left(m_v a_x + F_{Aerodrag} + 2m_{RF}a_x + J_{z1}\left(\frac{\ddot{\theta}_{11}}{R_1} + \frac{\ddot{\theta}_{12}}{R_1}\right) + F_{RR11} + F_{RR12}\right)\gamma_j \quad (22)$$

Table 5 compares SMF* and OMF, for three values of γ_j.

Table 5. Comparison between SMF* and OMF for rear wheels - Acceleration

γ_j	SMF* term(s)	OMF term(s)	Magnitude
0	$-m_{RR}a_x$	0	|SMF*| > |OMF|
0.5	$-m_{RR}a_x - m_v a_x/2 - m_{RF}a_x$	$-m_{RR}a_x - m_v a_x/2 - m_{RF}a_x$	|SMF*| = |OMF|
1	$-m_{RR}a_x - m_v a_x - 2m_{RF}a_x$	$-2m_{RR}a_x - m_v a_x - 2m_{RF}a_x$	|SMF*| < |OMF|

During braking, again front and rear wheels need to be analyzed. For the front wheels Eq. (18) can be modified as:

$$F_{x1j} = -m_{RF}a_x + (-m_v a_x - F_{Aerodrag})\frac{\delta}{2} \quad (23)$$

Table 6 compares SMF* and OMF for the front wheels, for three values of δ.

Table 6. Comparison between SMF* and OMF for front wheels - Braking

δ	SMF* term(s)	OMF term(s)	Magnitude
0	$-m_{RF}a_x$	0	|SMF*| > |OMF|
0.5	$-m_{RF}a_x - m_v a_x/4$	$-m_{RF}a_x/2 - m_v a_x/4 - m_{RR}a_x/2$	|SMF*| ≠ |OMF|
1	$-m_{RF}a_x - m_v a_x/2$	$-m_{RF}a_x - m_v a_x/2 - m_{RR}a_x$	|SMF*| < |OMF|

For the rear wheels, Eq. (19) changes into:

$$F_{x1j} = -m_{RR}a_x + (-m_v a_x - F_{Aerodrag})\frac{(1-\delta)}{2} \quad (24)$$

Table 7 compares SMF* and OMF, for the rear wheels, for three values of δ.

Table 7. Comparison between SMF* and OMF - Rear wheels - Braking

δ	SMF*	OMF	Magnitude
0	$-m_{RR}a_x - m_v a_x/2$	$-m_{RR}a_x - m_v a_x/2 - m_{RF}a_x$	|SMF*| < |OMF|
0.5	$-m_{RR}a_x - m_v a_x/4$	$-m_{RR}a_x/2 - m_v a_x/4 - m_{RF}a_x/2$	|SMF*| ≠ |OMF|
1	$-m_{RR}a_x$	0	|SMF*| > |OMF|

When looking at acceleration (Table 5), again SMF* and OMF provide the same result only if $\gamma_j = 0.5$. Interestingly however, during braking (Tables 6 and 7, last column) SMF* and OMF provide different results even when $\delta = 0.5$.

4 Comparison among T.R.I.C.K. Formulation, SMF and OMF

The SMF and OMF, along with the T.R.I.C.K. formulation [9], were compared by means of experimental data, obtained on a professional proving ground with a high-performance vehicle (details on which cannot be disclosed). All the relevant parameters were available for the vehicle, except details on the front and rear unsprung masses. Only the average value of unsprung mass was available. Therefore it was not possible to study the performance of the SMF*.

Figure 5 shows a comparison between SMF and OMF considering the longitudinal forces obtained at each vehicle corner ij (indicated in the legend). The percentage error depicted in Fig. 5 is calculated as:

$$e_{SMF-OMF} = \frac{F_{xij,SMF} - F_{xij,OMF}}{F_{xij,SMF}} 100 \tag{25}$$

According to Fig. 5, the error between the SMF and OMF reaches up to 10%.

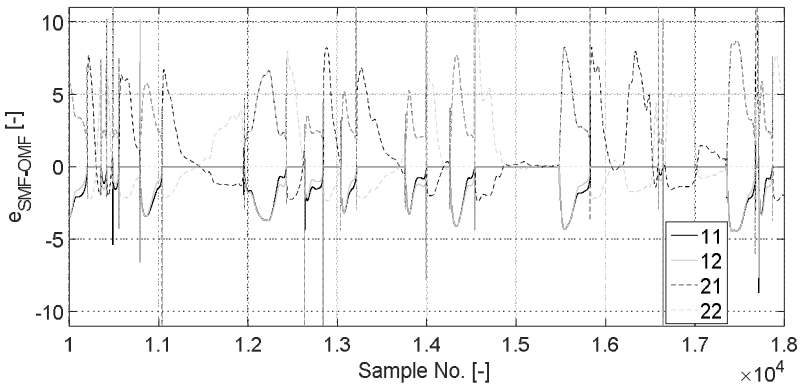

Fig. 5. Percentage error between SMF and OMF for the four wheels

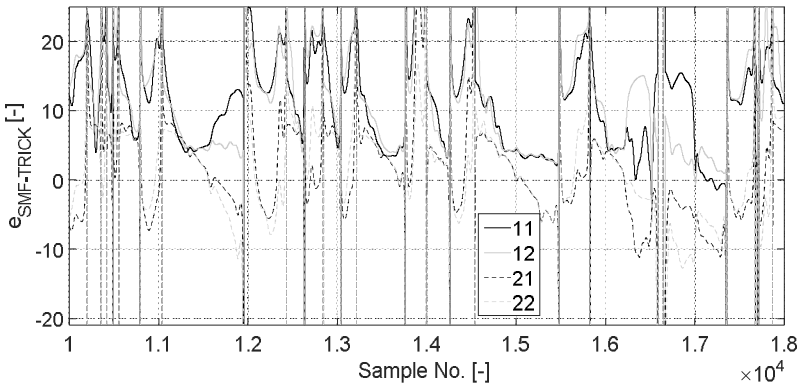

Fig. 6. Percentage error between SMF and T.R.I.C.K. formulation for the four wheels

Figure 6 compares, in a similar fashion, the SMF with the T.R.I.C.K. formulation. The percentage error depicted in Fig. 6 is calculated as:

$$e_{SMF-TRICK} = \frac{F_{xij,SMF} - F_{xij,TRICK}}{F_{xij,SMF}} 100 \quad (26)$$

In this case the error is up to 20%, and in general it is often different from zero.

5 Conclusion

In this paper three different formulations (SMF, SMF* and OMF) were presented within a new approach for the estimation of the tire-road longitudinal forces of a race car. The proposed approach is generally based on the equilibrium equations of front and rear sprung masses, along with the equilibrium equations of the unsprung mass. Moreover, the knowledge of the vehicle sprung/unsprung mass distribution improves the estimation of longitudinal forces up to 10% compared to when such specific piece of information is not available. Also, when comparing the SMF with the T.R.I.C.K. formulation, differences are up to 20%.

Future studies will involve: i) the availability of specific information on the front and rear unsprung masses, which allows to experimentally validate the SMF*; ii) the adoption of advanced sensors on the test vehicle, such as driveshaft load cells, wheel force transducers, brake pressure sensors. That would allow to further validate the proposed approach, which ultimately is meant to be an useful tool for motorsport and race engineers to investigate the vehicle behavior in a simple yet effective fashion.

References

1. Guiggiani, M.: The science of vehicle dynamics. 2nd edn. Springer, Pisa, Italy (2018).
2. Wong, J. Y.: Theory of ground vehicles. 4th edn. John Wiley & Sons, New York, USA (2008).
3. Rajamani, R.: Vehicle dynamics and control. 2nd edn. Springer, New York, USA (2011).
4. Meywerk, M.: Vehicle dynamics. 1st edn. John Wiley & Sons (2015).
5. Lenzo, B., Bucchi, F., Sorniotti, A., Frendo, F., On the handling performance of a vehicle with different front-to-rear wheel torque distributions. Vehicle System Dynamics, in press (2018).
6. Acosta, M., Kanarachos, S.: Tire lateral force estimation and grip potential identification using Neural Networks, Extended Kalman Filter, and Recursive Least Squares. Neural Computing and Applications, 1-21 (2017).
7. Dakhlallah, J., Glaser, S., Mammar, S., Sebsadji, Y.: Tire-road forces estimation using extended Kalman filter and sideslip angle evaluation. In AMERICAN CONTROL CONFERENCE 2008, IEEE, pp. 4597-4602 (2008).
8. Chindamo, D., Lenzo, B., Gadola, M.: On the vehicle sideslip angle estimation: a literature review of methods, models, and innovations. Applied Sciences, 8(3), p.355 (2018).
9. Farroni, F.: TRICK-Tire/Road Interaction Characterization & Knowledge - A tool for the evaluation of tire and vehicle performances in outdoor test sessions. Mechanical Systems and Signal Processing 72, 808-831 (2016).
10. Duarte, F., Ferreira, A., Fael, P. Software tool for simulation of vehicle–road interaction. Engineering Computations 34(5), 1501-1526 (2017).